Received: 31 May 2019 | Revised: 18 October 2019 | Accepted: 11 November 2019

DOI: 10.1002/ajh.25679

RESEARCH ARTICLE

AJH WILEY

Impact of natural neuromedin-B receptor variants on iron metabolism

Raffaela Rametta[1] | Paola Dongiovanni[1] | Guido A. Baselli[2] | Serena Pelusi[2,3] | Marica Meroni[1] | Anna L. Fracanzani[1,2] | Fabiana Busti[4] | Annalisa Castagna[4] | Stefania Scarlini[5] | Elena Corradini[5] | Antonello Pietrangelo[5] | Domenico Girelli[4] | Silvia Fargion[1,2] | Luca Valenti[2,3]

[1]General Medicine and Metabolic Diseases, Fondazione IRCCS Ca' Granda Ospedale Maggiore Policlinico, Milan, Italy

[2]Department of Pathophysiology and Transplantation, Università degli Studi di Milano, Milan, Italy

[3]Translational Medicine – Department of Transfusion Medicine and Hematology, Fondazione IRCCS Ca' Granda Ospedale Maggiore Policlinico, Milan, Italy

[4]Department of Medicine, Section of Internal Medicine, Azienda Ospedaliera Universitaria Integrata Verona, University of Verona, Verona, Italy

[5]Internal Medicine and Center for Hemochromatosis and Heredometabolic Liver Diseases, Azienda Ospedaliera Universitaria di Modena, University of Modena and Reggio Emilia, Modena, Italy

Correspondence
Luca Valenti, Translational Medicine – Department of Transfusion Medicine and Hematology, Fondazione IRCCS Ca' Granda Ospedale Maggiore Policlinico, Department of Pathophysiology and Transplantation, Università degli Studi di Milano, Padiglione Marangoni, Ospedale Policlinico via F Sforza 35, 20 122 Milano (MI), Italy.
Email: luca.valenti@unimi.it

Funding information
Associazione Italiana per la Ricerca sul Cancro, Grant/Award Number: MyFirst Grant AIRC n.16888; Associazione Malattie Metaboliche del Fegato; Fondazione Italiana per la Ricerca in Epatologia - FIRE; Horizon 2020 Framework Programme, Grant/Award Number: 777377; Horizon 2020; European Union; Ministero della Salute, Grant/Award Number: Ricerca Finalizzata Ministero della Salute RF-2016

Abstract

Iron overload heritability remains partly unexplained. By performing whole exome sequencing in three patients with a clinical phenotype of hemochromatosis not accounted by known genetic risk factors, we identified in all patients rare variants predicted to alter activity of Neuromedin-B receptor (NMBR). Coding *NMBR* mutations were enriched in 129 patients with hereditary hemochromatosis or iron overload phenotype, as compared to ethnically matched controls, including 100 local healthy blood donors and 1000Genomes project participants (15.5% vs 5%, P = .0038 at burden test), and were associated with higher transferrin saturation in regular blood donors (P = .04). Consistently, in 191 patients with nonalcoholic fatty liver, the most common low-frequency p.L390 M variant was independently associated with higher ferritin (P = .03). In 58 individuals, who underwent oral iron challenge, carriage of the p.L390 M variant was associated with higher transferrin saturation and lower hepcidin release. Furthermore, the circulating concentration of the natural NMBR ligand, Neuromedin-B, was reduced in response to iron challenge. It was also decreased in individuals carrying the p.L390 M variant and with hemochromatosis in parallel with increased transferrin saturation. In mice, *Nmbr* was induced by chronic dietary iron overload in the liver, gut, pancreas, spleen, and skeletal muscle, while *Nmb* was downregulated in gut, pancreas and spleen. Finally, *Nmb* amplified holo-transferrin dependent induction of hepcidin in primary mouse hepatocytes, which was associated with *Jak2* induction and abolished by the NMBR antagonist PD168368. In conclusion, *NMBR* natural variants were enriched in patients with iron overload, and associated with facilitated iron absorption, possibly related to a defect of iron-induced hepcidin release.

1 | INTRODUCTION

Hereditary hemochromatosis (HH) is characterized by excessive iron absorption not accounted for by enhanced erythropoiesis, leading to parenchymal accumulation and organ damage with hepatic and extra-hepatic complications.[1] This endocrine disorder is due to a deficit in production and/or in the activity of hepcidin,[2] the hepatic hormone that prevents un-needed iron from entering the bloodstream. This goal is achieved by inducing the internalization and degradation of the iron exporter ferroportin (FPN1)[3] or, independently of the endocytosis mechanism, by occluding FPN1 main cavity.[4]

Known causes of HH include mutations in upstream regulators of the expression of hepcidin, including *HFE*, *Transferrin receptor-2* (*TFR2*), *Hemojuvelin* (*HJV*) or the disruption of the *Hepcidin* gene (*HAMP*) itself and its target *FPN1*. Recently, mutations in the pro-peptide sequence of *Bone Morphogenic Protein-6* (*BMP6*), resulting in a reduced ability to promote hepcidin expression, have also been proposed as a new cause of hereditary iron overload resembling HH.[5,6]

Homozygosity for the p.C282Y variant of *HFE* is the most common cause of HH (*HFE*-related or classical hemochromatosis), accounting for about 69% of cases in Italy and Southern Europe.[7] Rare genetic variants in *TFR2*, *HJV*, *HAMP*, *FPN1* or *BMP6* only account for a limited number of the remaining cases.[8] Moreover, the penetrance and phenotypic expression of homozygosity for the p.C282Y *HFE* variant is variable, but more consistent within families, suggesting an influence by still unidentified genetic modifiers.[9]

Genome-wide association studies for iron related traits led to the identification of common single nucleotide polymorphisms (SNPs) explaining a fraction of iron traits variability at population level. In particular, the p.A736V variant in *Matriptase-2* (*TMPRSS6*) was associated with iron deficiency and hepcidin modulation in the general population,[10,11] as well as with the penetrance of HH in patients from Northern Italy.[12] Recently, the p.D519G variant in *Glyceronephosphate O-Acyltransferase* (*GNPAT*) has been proposed as a modifier of *HFE* P.C282Y expression and associated with severe iron overload in p.C282Y homozygous patients.[13] However, the impact of these variants on the predisposition to primary iron overload is still controversial.[14,15]

By exploiting next generation whole exome sequencing of patients with unexplained iron overload, here we identified *Neuromedin B receptor* (*NMBR*) as a novel candidate gene regulating iron metabolism. We showed that rare variants in *NMBR* are enriched in HH and iron overload syndromes. Furthermore, functional studies suggested that NMBR is involved in the regulation of hepcidin secretion in response to increased transferrin saturation.

2 | METHODS

2.1 | Patients

Primary iron overload phenotype was defined by increased ferritin (>500 ng/mL) and transferrin saturation (TS%, >50) and presence of parenchymal siderosis assessed by histology or magnetic resonance imaging, not explained by excess alcohol intake, iron supplementation, chronic transfusion or hematological disorders. Other causes of liver disease alpha1-antitrypsin deficiency, chronic viral and autoimmune hepatitis and Wilson disease were also ruled out.

Hereditary hemochromatosis was diagnosed in patients with primary iron overload when pathogenic mutations in causal genes were detected in homozygosity or compound heterozygosity.

2.1.1 | Discovery cohort

Whole exome sequencing (WES) was performed on DNA extracted from the peripheral blood of three unrelated patients with unexplained iron overload diagnosis. This is suggestive of HH, where mutations in known risk loci and acquired risk factors could not explain the severity of iron overload, and patients were treated at Hepatology Outpatient Service of Fondazione IRCCS Cà Granda Ospedale Maggiore Policlinico of Milan. Table S1 summarizes their clinical features.

2.1.2 | Primary iron overload cohort

To replicate the WES findings, we considered 129 unrelated patients (105 consecutive unselected probands from Milan and 24 from Verona and Modena[16]) with primary iron overload phenotype. Of these patients, 44 carried the p.C282Y mutation in homozygosity, while 85 was negative for *HFE* genotypes predisposing to iron overload.

We also considered 100 Italian regular blood donors with normal serum ferritin and transferrin saturation (TS%) at first blood donation, of similar sex and age distribution to the controls. Clinical features and the *HFE* genotype of the subjects included are shown in Table S2.

2.1.3 | NAFLD cohort

To evaluate whether *NMBR* risk variants impact on iron metabolism in other liver diseases characterized by alteration of iron homeostasis, we considered 191 Italian patients with a histologic diagnosis of non-alcoholic fatty liver disease (NAFLD), with complete characterization of circulating and hepatic iron,[17] without HH (Table S3). Circulating ferritin was selected as main outcome, because is a marker of hepatic iron stores in this condition.[18] Hyperferritinemia was defined for values of serum ferritin >240/320 ng/mL in women/men.

2.1.4 | Oral iron tolerance test cohort

We considered 64 subjects, whose iron homeostasis was studied by oral iron tolerance test (OITT) with serum hepcidin measurement at baseline and at 4, 8, and 24 hours after the administration of 105 mg of ferrous sulfate.[19] Ten out of 64 had p.C282Y *HFE* +/+ HH, while the remaining 54 were subjects with normal TS% and wild type for

p.C282Y *HFE*; five of them carried the p.L390M variant of *NMBR*. Table 1 shows demographic and clinical features of the OITT cohort.

The study was approved by the institutional Review Board of the Fondazione IRCCS Ca' Granda, and was conducted according to the principles of the Declaration of Helsinki. All evaluated subjects signed an informed consent.

2.2 | Genetic analysis

2.2.1 | DNA samples collection and extraction

The DNA samples were extracted from the peripheral blood by standard phenol-chloroform protocol. Quality control was be performed by evaluating the 260/280 nM absorbance ratio and gel electrophoresis.

2.2.2 | Whole exome sequencing

Whole exome sequencing was performed by array capture of 50 Mb of exome target sequence using the Agilent SureSelect Human All Exon V5 enrichment kit (Agilent, Santa Clara, CA) followed by paired-end sequencing (150 bases each read) on an Illumina HiSeq 4000 platform (Illumina, San Diego, CA).

Sequences were aligned to the human genome (GRCh37) using Burrows-Wheeler Aligner, v.0.7.10.[20] Base quality recalibration, indel realignment, and calling of SNVs and small indels were performed using the Genome Analysis Toolkit (GATK), v.3.3-0, as previously described.[21] Base quality score recalibration, indel realignment, duplicate removal, and SNP and indel discovery were performed simultaneously using standard hard filtering parameters or variant quality score recalibration according to GATK Best Practices recommendations.[22,23] Variants were annotated using Variant Effect predictor (VEP)[24] with gene annotations made according to ENSEMBL transcripts release 89. Previously known variants were annotated with their allele frequencies from the 1000 Genomes Project,[25] the Exome Aggregation Consortium (ExAC) release 0.3 and the Genome Aggregation Database (gnomAD) release 2.0.[26] Variants were filtered by using hard parameters (coverage ≥15X and mutation call quality ≥150).

We selected rare variants (MAF ≤0.001 gnomAD non-Finnish Europeans and 1000 Genomes Europeans), with a high likelihood to impact on the protein function predicted by a Combined Annotation Dependent Depletion (CADD) Phred score ≥40[27] and Deleterious Annotation of genetic variants using Neural Networks (DANN) score ≥0.9.[28] The bioinformatics pipeline is depicted in Figure S1.

2.2.3 | Sanger sequencing

The *NMBR* coding sequence and exons flanking regions were fully sequenced by Sanger's method. Briefly, all regions of interest were amplified by standard PCR protocol using suitable primers (Sigma Aldrich, St. Louis, MO, Exon 1: forward 5′- ACCTAAATCGTGGGCGTTC -3′ and reverse 5′- CACTCCGGGTGAGTCTTCTC -3′; Exon 2: forward 5′- CCAG GAACCTTAGGTCTTCCA –3′ and reverse 5′- TGAAGGCCCAACT CTGTTCT –3′; Exon 3: forward 5′- GGTATGTGGCTGGTTCCATT –3′ and reverse 5′- CATTGGTTTGGGGATCATCT –3′); cycle sequencing were performed using Big Dye terminator v1.1 cycle sequencing kit, and run on 310 Genetic Analyzer (Life Technologies-Thermofisher Scientific, Carlsbad, CA).

TABLE 1 Demographic and clinical features of OITT cohort stratified according to HFE genotype and impact of the p.L390M *NMBR* variant on iron metabolism during OITT in 54 individuals without HH diagnosis

	***HFE* p.C282Y +/+**				
	NO			**YES**	***P***
Gender, F (%)	36			30	
Age, years	45 ± 17			47 ± 20	.9
Ferritin at diagnosis, ng/mL	126 {64-617}			514 {304-934}	.0003
TS% at diagnosis	30 ± 10			80 ± 12	<.0001
***NMBR* p.L390M**	**CC (n = 49)**	**CA (n = 5)**	***P****	**CC + CA (n = 10)**	***P***
AUC S-iron	2750 ± 844	4016 ± 741	0.002	4521 ± 810	<.0001
AUC TS%	716 ± 205	1057 ± 192	0.0006	1595 ± 264	<.0001
AUC Hepcidin	296 ± 114	294 ± 97	0.97	113 ± 59	<.0001
HRL	0.43 ± 0.23	0.26 ± 0.12	0.033	0.07 ± 0.04	<.0001
Baseline FT, ng/mL	103 {60-138}	53 {34-136}	0.32	35 {29-49}	<.0001

Note: Values are reported as mean ± SD, median {IQR}, or number (%), as appropriate. Demographical features and iron parameters of patients were compared between *HFE* C282Y genotypes using linear regression model (for continuous characteristics) or logistic regression model (for categorical characteristics). *P** = *P* value p.L390M CA vs CC genotype. CC genotype encodes for p.L390M wild type variant; CA genotype encodes for p.L390M +/– variant.

Abbreviations: AUC S-Iron, Serum iron area under curve; AUC TS%, transferrin saturation % area under curve; AUC Hepcidin, serum hepcidin area under curve; HRL, hepcidin release index = serum hepcidin 8 hours/TS% 4 hours; FT, ferritin; +, homozygous mutant variant.

2.2.4 | Genotyping of p.L390 M variant

The *NMBR* rs7453944C>A SNP (p.L390M variant) was determined by sequence allele specific PCR, using two allele-specific primers, that differ by a single nucleotide corresponding to the polymorphic nucleotide (C or A), and a common reverse primer in separate reactions. The primer sequences were as follows: common reverse 5′- AGC AAGTTCTGATCTGCCGA –3′, allele C specific forward 5′-CATGAA GCAGGAAATGGCAC-3′, allele A specific forward 5′- CATGA AGCAGGAAATGGCAA-3′.

2.3 | Neuromedin B measurement

Serum Neuromedin B (NMB) was assessed by human NMB ELISA kit (Cloud-Clone Corp., Katy, TX): a solid phase enzyme-linked immunosorbent assay based on the principle of competitive binding, according to manufacturer instruction. The assay sensitivity was lower than 49.3 pg/mL and intra-assay precision was more than 90%. Samples optical density was determined at 450 nm with Infinite F200 pro Tecan microplate reader (Tecan Group Ltd, Männedorf, Switzerland). All samples were measured in duplicates.

2.4 | Hepatocyte isolation and in vitro experiments

Hepatocytes were isolated from six-week-old male C57Bl/6 mice (Charles River, Calco, Italy; from n = 3 animals) by a multi-step ethylene glycol tetra-acetic acid (EGTA)/collagenase perfusion technique. This was through micro-cannulation of the portal vein to ensure efficient perfusion of tissue samples, as previously described.[29] Cells were plated 250 000/well on plastic six-well plates and cultured in DMEM medium supplemented with 10% FBS, 2 mM L-glutamine, 100 units/mL penicillin, 0.1 mg/mL streptomycin, 100 nM insulin and 100 nM dexamethasone.

After overnight starvation in DMEM-0.5% FBS, L-glutamine and antibiotics, hepatocytes were treated with holo-transferrin at 10 mg/mL and/or Neuromedin-B at 1 μM (Sigma Aldrich, St. Louis, MO) and/or NMBR antagonist PD168368 at 30 μM[30] (Cayman Chemical, Ann Arbor, MI). After 1, 4 and 8 hoursours since treatments, cells were harvested in Trizol reagent (Life Technologies-Thermofisher Scientific, Carlsbad, CA) for RNA extraction.

Holo-transferrin and NMB were dissolved in water, and added to each well at a concentration of 10 mg/mL and 1 μM, respectively. The NMBR antagonist PD168368 was dissolved in DMSO and administered to cells to a final concentration of 30 μM.

HepG2 cells were cultured in in DMEM medium supplemented with 10% FBS, 2 mM L-glutamine, 100 units/mL penicillin, 0.1 mg/mL streptomycin. After overnight starvation in DMEM-0.5% FBS, L-glutamine and antibiotics, HepG2 were treated with ferric ammonium citrate (FAC) 150 μM for 24 hours and harvested in Trizol reagent for RNA extraction.

2.5 | In vivo experiments

The in vivo models of iron-enriched and standard diet (IED and SD) have been described in details in a previous publication.[31] Briefly, tissues isolated from six-week-old male C57Bl/6 mice (Charles River, Calco, Italy), housed at constant room temperature (23°C) under 12-hour light/dark cycles with ad libitum access to water in compliance with the Principles of Laboratory Animal Care (NIH publication 86-23). and the mice were fed either a standard iron concentration diet (8 mg/kg; control, measured by atomic absorption spectrometry in a regular commercial chow diet; n = 3) or an iron-enriched diet (IED; 3% carbonyl-iron, a highly pure form of iron, which does not contain carbohydrates; n = 3) for 16 weeks.[31]

2.6 | Gene expression analysis

Quantitative real time PCR (qRT-PCR) was performed by the ABI 7500 fast thermocycler (Life Technologies-Thermofisher Scientific, Carlsbad, CA), using Taqman gene expression assays (Life Technologies-Thermofisher Scientific, Carlsbad, CA). All reactions were delivered in triplicate. Data were normalized to the β-actin gene expression and results were expressed as arbitrary units.

2.7 | Statistical analysis

For descriptive statistics, continuous traits were summarized as means±SD. Serum ferritin and hepcidin levels were summarized as median and interquartile range. Categorical variables were shown as percentages. Multivariate analyses were performed by fitting data to generalized linear regression models, adjusted for relevant covariates as detailed in the results section.

Analyses were conducted with the JMP 13.0 statistical analysis software (SAS Institute, Cary, NC). Differences were considered significant when $P < .05$ (two tailed).

3 | RESULTS

3.1 | *NMBR* mutations are enriched in patients with primary iron overload

From whole exome sequencing data, we selected genes carrying at least one variant that was rare (allelic frequency ≤ 0.001) and predicted to impact on protein function (CADD Phred ≥40 and DANN score ≥ 0.9). Among the identified candidate genes, *NMBR* was the only one mutated in all patients: two carried the p.C318Y and p.L390M *NMBR* mutations in heterozygosity, while one carried the p.E252*fs and p.L390M variants in compound heterozygosity. The *NMBR* mutations identified in the discovery group are presented in Table S4.

In order to validate the association between *NMBR* variants and iron overload, we sequenced *NMBR* coding sequence and exons

TABLE 2 Frequency of rare mutations altering NMBR protein sequence and association with HH

Variant	rs	Chr position	IO-Pt overall N = 129	Healthy blood donors N = 100	1000G EUR	gnomAD NFE	OR {95% CI}
p.C318Y	rs41289827	142 397 005	5 (0.038)	1(0.01)	0.005	0.0031	vs healthy blood donors[a] 3.1 {1.1-8.9} ***P* = .02**
E252*fs	rs145581958	142 399 709	1 (0.008)	0(0)	0.001	0.0005	
p.L40V	Novel	142 409 678	0 (0)	1(0.01)	N/A	-	
p.P148H	rs138994608	142 400 020	8 (0.06)	1 (0.01)	0.024	0.032	
p.I167V	rs56126862	142 399 964	2 (0.015)	1 (0.01)	0.0002	0.0032	vs 1000G[a] 3.6 {1.8-7.4} ***P* = .005**
p.A243T	rs147317413	142 399 736	1 (0.008)	0 (0)	0.0002	0.0002	
p.R310W	rs142626832	142 397 030	2 (0.015)	1 (0.01)	0.0028	0.006	
p.S357T	Novel	142 396 889	1 (0.008)	0 (0)	N/A	-	
Variant	**rs**	**Chr position**	**IO-Pt p.C282Y +/+ N = 44**	**Healthy blood donors N = 100**	**1000G EUR**	**gnomAD NFE**	**OR {95% CI}**
p.C318Y	rs41289827	142 397 005	1 (0.02)	1 (0.01)	0.005	0.0031	vs healthy blood donors 3.5 {1.04-11.7} ***P* = .04**
p.E252*fs	rs145581958	142 399 709	0 (0)	0 (0)	0.001	0.0005	
p.L40 V	Novel	142 409 678	0 (0)	1 (0.01)	N/A	-	
p.P148H	rs138994608	142 400 020	4 (0.09)	1 (0.01)	0.024	0.032	
p.I167V	rs56126862	142 399 964	2 (0.02)	1 (0.01)	0.0002	0.0032	vs 1000G 2.7 {1.1-7.2} ***P* = .04**
p.A243T	rs147317413	142 399 736	1 (0.02)	0 (0)	0.0002	0.0002	
p.R310W	rs142626832	142 397 030	0 (0)	1 (0.01)	0.0028	0.006	
p.S357T	Novel	142 396 889	1 (0.02)	0 (0)	N/A	-	
Variant	**rs**	**Chr position**	**IO-Pt p.C282Y −/− N = 85**	**Healthy blood donors N = 100**	**1000G EUR**	**gnomAD NFE**	**OR {95% CI}**
p.C318Y	rs41289827	142 397 005	4 (0.047)	1 (0.01)	0.005	0.0031	vs healthy blood donors 3.4 {1.1-10.1} ***P* = .025**
p.E252*fs	rs145581958	142 399 709	1 (0.018)	0 (0)	0.001	0.0005	
p.L40V	Novel	142 409 678	0 (0)	1 (0.01)	N/A	-	
p.P148H	rs138994608	142 400 020	4 (0.047)	1 (0.01)	0.024	0.032	
p.I167V	rs56126862	142 399 964	0 (0)	1 (0.01)	0.0002	0.0032	vs 1000G 3.2 {1.5-6.6} ***P* = .0019**
p.A243T	rs147317413	142 399 736	0 (0)	0 (0)	0.0002	0.0002	
p.R310W	rs142626832	142 397 030	2 (0.02)	1 (0.01)	0.0028	0.006	
p.S357T	Novel	142 396 889	0 (0)	0 (0)	N/A	-	

[a]Logistic regression models were used to test the association adjusted for *HFE* p.C282Y genotype. Chr position: Chromosome position; C282Y −/−: p.C282Y genotype wild-type; C282Y +/+: p.C282Y genotype mutated in homozygosity. Frequency of heterozygous subjects is indicated in parentheses. Iron overload (IO)-Patients included both HH (homozygous for p.C282Y *HFE* mutant variant) and primary iron overload patients.

flanking regions in 129 hemochromatosis phenotype patients (both HH and primary iron overload), who were compared to 100 regular blood donors with normal iron parameters. Results are shown in Table S5. We confirmed an enrichment in rare *NMBR* coding variants in primary iron overload patients, as compared to healthy individuals (prevalence 15.5% vs 5%, respectively, $P = .0038$ at Burden test). At multivariate logistic regression analysis, carriage of *NMBR* mutations was associated with higher risk of iron overload independently of BMI, presence of *HFE* genotypes at risk, and of the *TMPRSS6* p.A736V variant (OR 3.1, 95% c.i. 1.1-8.9, $P = .02$; Table 2). Notably, we found a significant enrichment in *NMBR* mutations in both patients with classic HH and in those with other iron overload syndromes ($P < .05$ vs both local controls and healthy individuals of 1000Genomes project).

Table S6 summarizes iron parameters in the evaluated individuals stratified by the presence of *NMBR* mutations. In regular blood donors, carriage of *NMBR* mutations was associated with both higher circulating iron (median 117 IQR (104-143) vs 84 (58-118) in carriers vs non-carriers, $P = .035$) and TS% (33 (26-42) vs 23 (14-30), $P = .04$).

3.2 | The p.L390M *NMBR* variant is associated with ferritin levels in NAFLD

In order to validate the impact of *NMBR* variation on iron status in other liver diseases associated with altered iron metabolism, we genotyped NAFLD patients for the p.L390M variant, the most common missense *NMBR* mutation in the European population. Carriers of the p.L390M variant had higher circulating ferritin concentration as compared to non-carriers (307 (170-751) vs 277 (138-573), respectively; $P = .047$). By multivariate analysis, carriage of the p.L390M variant was associated with ferritin independently of age, sex, BMI, presence of *HFE* genotypes at risk, and of the *TMPRSS6* p.A736V variant ($P = .03$, Table S7).

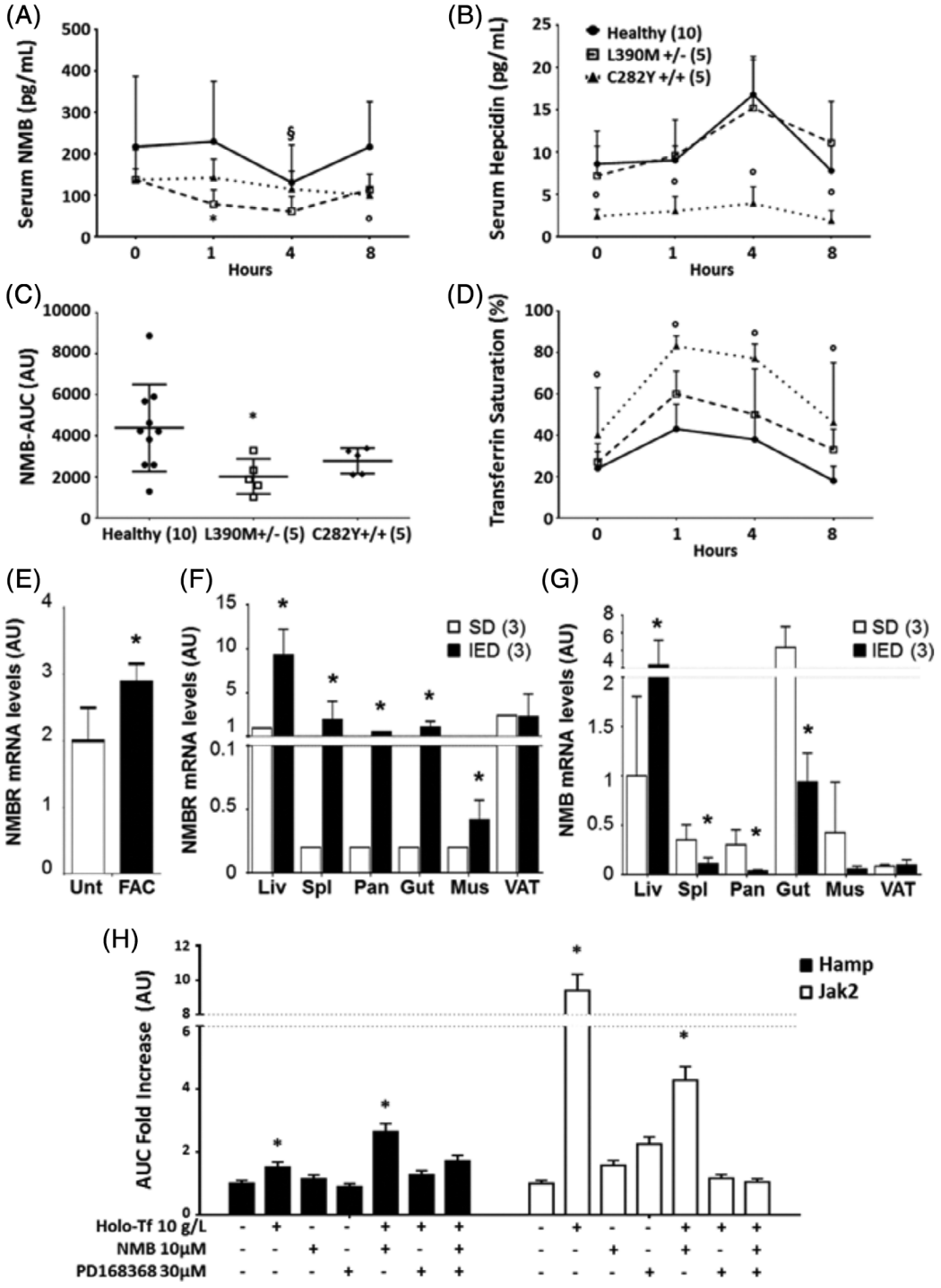

FIGURE 1 Impact of *NMBR* p.L390M variant on circulating Neuromedin B (NMB), hepcidin and transferrin saturation levels in individuals underwent to oral iron tolerance test and iron mediated NMBR and NMB modulation *in vitro* and *in vivo*. NMB (Panel A), hepcidin serum levels (Panel B), area under the curve of serum NMB (Panel C), Transferrin saturation (Panel D) at baseline and after 4, 8 and 24 hours after oral administration of 105 mg iron sulfate. Solid line: wild-type healthy volunteers with normal iron parameters (n = 10); dotted line: HH patients carrying p.C282Y *HFE* variant in homozygosity (n = 5); dashed line: subjects carrying the p.L390M *NMBR* variant in heterozygosity (n = 5; $*P < .05$ in p.L390M+/– vs healthy; $°P < .05$ in p.C282Y+/+ vs healthy; $^{§}P < .05$ vs baseline). Iron induced *NMBR* expression in HepG2 cells treated with 150 µM of ferric ammonium citrate for 24 hours (FAC; *: $P = .04$ vs untreated, unt, Panel E) and in tissues of mice fed with standard (SD, withe bar) or iron enriched diet (IED, black bar; Panel F and G *:$P < .05$). Both NMBR and NMB expression were evaluated by qRT-PCR. All samples were done in triplicate and normalized for beta-actin. Panel A shows the mean of three in vitro experiments. Panel B and C summarize the mean of *NMBR* and *NMB* gene expression of three mice per group (SD or IED) expressed as fold increase vs SD. Comparisons were performed by Student *t* test. In primary hepatocytes, iron supplementation induced *Hamp* and *Jak2* gene expression (Panel H; $*P < .05$ vs vehicle); NMB treatment amplified transferrin-induced *Hamp* expression and upregulated *Jak2* gene expression ($*P < .05$ vs vehicle). Inhibition of Nmbr by PD138368 abrogated iron-mediated *Hamp* and *Jak2* expression. Figures are representative of three biological replicates. Comparisons were performed by Student *t* test. AUC, Area Under the Curve; AU, Arbitrary units

3.3 | Impact of p.L390M *NMBR* variant on iron metabolism during OITT

In individuals without HH and normal iron stores who underwent OITT, both serum iron and TS% areas under the curve (AUCs) were higher in subjects carrying the p.L390M variant (n = 5) as compared to non-carriers (n = 53; s-iron-AUC 4016 ± 741 vs 2750 ± 844, respectively, P = .002; TS%-AUC 1057 ± 192 vs 716 ± 205, respectively, P = .0006). The Hepcidin Release Index (HRL = serum hepcidin at 8 hours/TS%[19] at 4 hours, corresponding to hepcidin and TS% peaks, respectively) was lower in patients carrying p.L390M variant as compared to non-carriers (0.26 ± 0.12 vs 0.43 ± 0.23, respectively, P = .033; Table 1). These data are consistent with a slight deficit in hepcidin secretion in carriers of the p.L390M *NMBR* variant, leading to mildly increased iron absorption and TS% after iron-containing meals, and subsequently to a restoration of a "normal" hepcidin response limiting iron absorption, though at a higher TS% threshold.

3.4 | Circulating neuromedin B is modulated by iron status

In order to evaluate whether iron administration may affect the release of the NMBR natural ligand Neuromedin B (NMB), we measured NMB serum levels in 10 healthy individuals negative for the p.L390 M variant, five carriers of the p.L390 M variant without HH, and five HH patients, who underwent OITT. Circulating NMB was modulated by iron administration, as it decreased at 8 hours after iron challenge in healthy subjects (P = .004 at 8 h vs baseline; Figure 1A), concomitantly with the increase in circulating hepcidin (Figure 1B). Furthermore, HH patients had reduced circulating NMB as compared to healthy subjects, starting from baseline and for the entire duration of the test, and failed to show any significant modulation of NMB levels (Figure 1A).

Moreover, non-HH subjects carrying the *NMBR* p.L390M variant showed lower NMB level as compared to wild-type non-HH individuals with significant differences at 4 and 24 hours following iron challenge (142 ± 45 vs 211 ± 150, P = .04 and 114 ± 37 vs 199 ± 117, P = .05, respectively). The NMB-AUC was 50% higher in wild-type vs p.L390M carriers in non-HH individuals (P = .03; Figure 1C).

These data suggest that circulating NMB concentration is down-modulated during iron absorption, in the presence of homozygosity for the p.C282Y *HFE* mutation and by the p.L390M *NMBR* variant during OITT, concomitantly with an increase in circulating iron (Figure 1D).

3.5 | Iron modulates expression of NMBR and NMB in HepG2 cell line and in mouse tissues

To determine whether iron modulates *NMBR* expression, we evaluated mRNA levels first *in vitro* in human HepG2 hepatoma cell line exposed or not to 150 μM ferric ammonium citrate (FAC), and then *in vivo* in tissues of mice fed with standard (SD) or iron enriched diets (IED). The FAC treatment induced *NMBR* gene expression approximately by 1.5-fold in HepG2 (Figure 1E). Consistently, in mice *NMBR* was induced by chronic dietary iron overload in the liver, spleen and gut (Figure 1F), while *NMB* was downregulated by dietary iron in the gut, pancreas, and the spleen (Figure 1G).

3.6 | NMB amplifies HAMP induction by holo-transferrin in primary mouse hepatocytes in a NMBR dependent fashion

In order to test the impact of *NMB-NMBR* axis activation on hepcidin expression (*Hamp* gene), we exposed primary hepatocytes isolated from C57Bl/6 male mice to NMB and/or holo-transferrin and/or NMBR antagonist PD168368 and/or vehicle for 1, 4 and 8 hours. As expected, exposure to holo-transferrin upregulated *Hamp* mRNA levels at 4 hours as compared to the vehicle alone. Combined treatment with NMB amplified *Hamp* induction by holo-transferrin as early as 1 hour as compared to holo-transferrin alone (P = .004). Conversely, administration of NMBR antagonist PD168368 blunted the facilitating effect of NMB on holo-transferrin mediated *Hamp* induction (P = .002, Figure S2A). In order to determine which signal pathway was involved in *NMB-NMBR* mediated *Hamp* induction in this experimental setting, we evaluated the expression of *Bmp6-Smad4-TGFβ* and *Jak2-Stat3* and genes. Interestingly, unlike *Bmp6-Smad4*, and *TGFβ*, which did not showed any significant modulation by iron or NMB treatments (Figure S2C), *Jak2* gene expression followed the same pattern as *Hamp*. Indeed, *Jak2* is strongly induced by holo-transferrin administration. Combined treatment with NMB did not result in a further *Jak2* induction as compared to holo-transferrin, while the administration of NMBR antagonist PD168368 resulted in the down-modulation of *Jak2* expression to the baseline levels in cells exposed to holo-transferrin (Figure S2B).

As summarized by AUCs (Figure 1H), these data suggest that activation of the NMB-NMBR axis amplifies hepcidin production in response to rising circulating iron and that this effect is likely mediated by *Jak2* activation. Conversely, lack of *NMBR* activation in carriers of loss-of-function mutations may facilitate iron accumulation by down-modulating hepcidin production in response to iron challenge, at least in in those subjects with other iron overload triggering factors.

4 | DISCUSSION

In this study, we aimed to identify new genetic loci associated with regulation of iron metabolism. To this end, we first screened by whole exome sequencing a small number of individuals with unexplained iron overload, and found rare naturally occurring variants predicted with a high confidence to alter protein activity in the *NMBR* gene. Secondly, we validated the enrichment in rare *NMBR* variants in a larger cohort of patients with primary iron overload phenotype, as compared to both local controls with normal iron metabolism and healthy individuals from the 1000G project. We

confirmed that carriage of *NMBR* mutations in a heterozygous state determined an about 3-fold increase in the risk of developing iron overload. Notably, in regular blood donors with depleted iron stores, those positive for *NMBR* variants had increased TS%. Furthermore, the most common p.L390M *NMBR* variant (carried by about 8% of healthy European individuals, mostly on chromosomes 6 negative for the p.C282Y and p.H63D *HFE* variants), was associated with higher ferritin levels in patients with NAFLD, which are predisposed to develop iron metabolism alterations, and with increased iron absorption during OITT. Taken together, these data suggest that *NMBR* variants may predispose to iron accumulation due to facilitation of iron absorption.

Such as *HFE*, the human *NMBR* gene is localized at chromosome 6 and encodes for a 390 AMino acids receptor coupled to G protein and to the phospholipase C (PLC)/protein kinase C (PKC) signaling pathway. Note, NMBR activation leads also to stimulation of phospholipases A2 and D and extracellular signal-regulated protein kinase (ERK)/mitogen-activated protein kinase (MAPK).[32-36] The physiological functions regulated by NMBR in peripheral tissues include stimulation of smooth muscle contraction[37] and regulation of the pituitary gland.[38,39] NMBR is also expressed in the central nervous system, where it mediates the inhibition of food intake,[40,41] thermoregulation[42] and mediation of the stress and fear responses,[43] as well as various behaviors, such as spontaneous activity.[44] Thus, NMBR is involved in the regulation of cell growth and proliferation both in normal and neoplastic tissues.[45-47]

Despite NMBR and its natural ligand NMB have previously been involved in energy homeostasis,[38] and *NMB* has been identified as a candidate gene linking eating behaviors to obesity,[48] a possible contribution of NMBR in the regulation of iron metabolism was not previously hypothesized.

Prompted by the observed genetic association, we therefore examined the possible involvement of NMBR in the modulation of iron metabolism. In a cohort of individuals who underwent OITT, the

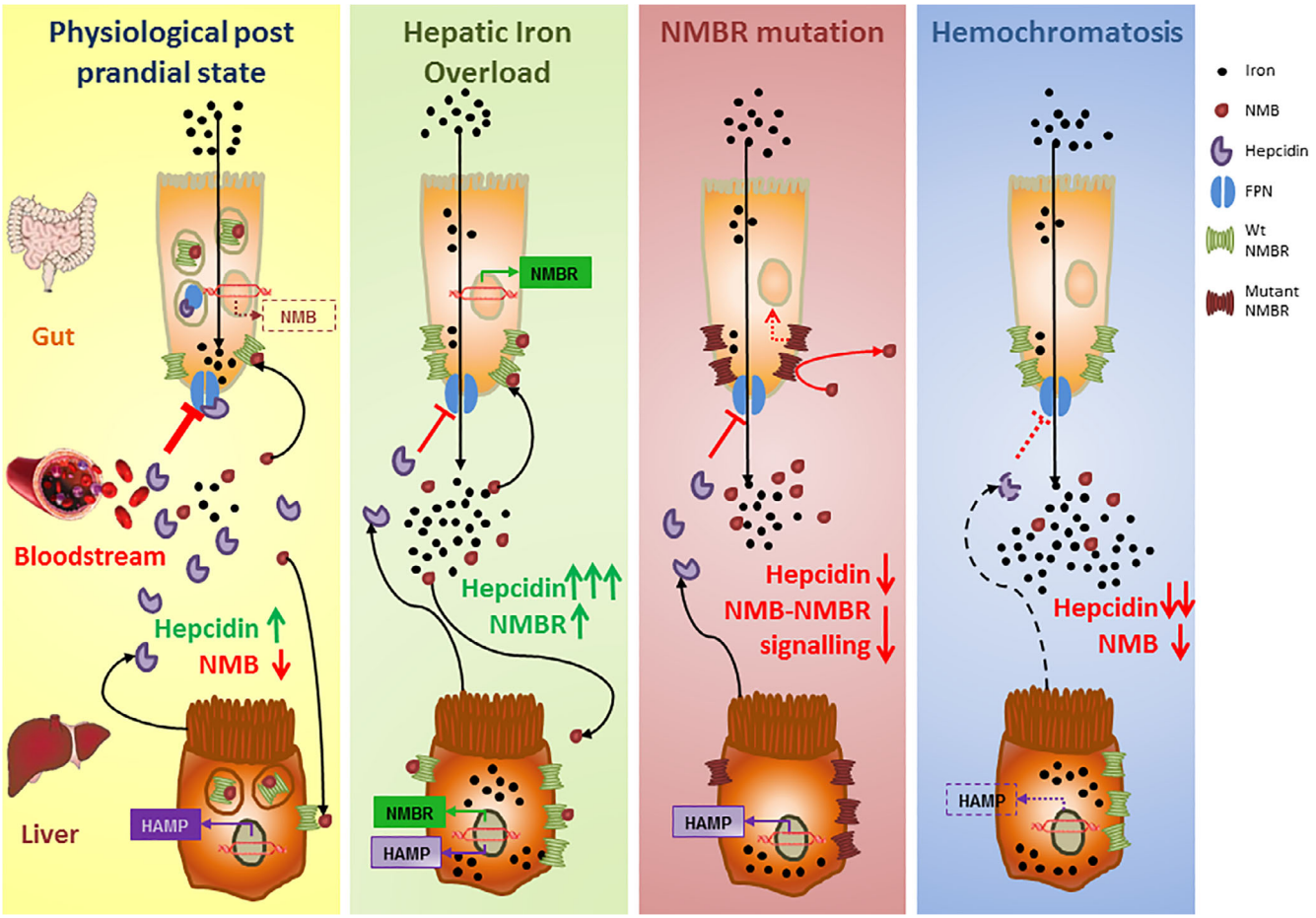

FIGURE 2 Hypothetical mechanisms explaining NMB-NMBR pathway involvement in the regulation of iron metabolism and pathogenesis of iron overload. In physiological conditions, during the post prandial state, NMB down-modulation limits hepcidin release allowing iron absorption from the gut (yellow panel). Conversely, in the presence of hepatic iron overload NMBR upregulation promotes HAMP transcription, thereby inhibiting further intestinal iron absorption and hepatic accumulation (green panel). When NMB-NMBR signal pathway is disrupted by the presence of *NMBR* loss of function mutations, hepcidin release is lower than in healthy subjects, predisposing to the development of an iron overloaded phenotype. In HH patients characterized by genetic deficit of hepcidin production, low circulating levels of NMB and/or disruption of NMB-NMBR signal pathway may contribute to iron overload (light blue panel). Dotted lines represent the down regulated pathways [Color figure can be viewed at wileyonlinelibrary.com]

release of hepcidin was slightly, but significantly reduced in carriers of the p.L390M *NMBR* variant (the most common variant resulting in an alteration of the protein in Europeans), while iron absorption was increased. These data suggest that *NMBR* variants facilitate iron absorption through down-modulation of hepcidin release in response to circulating iron.

In individuals without genetic predisposition to iron overload, oral iron challenge determined a reduction in circulating NMB. In line with these data, dietary iron overload determined a downregulation of *Nmb* expression in the gut, pancreas, and the spleen in mice. Although we could not evaluate Nmb secretion in mouse models of HH, in both p.C282Y$^{+/+}$ *HFE* HH patients and in p.L390M *NMBR* carriers, NMB was already downregulated at baseline. These data may suggest that increased iron availability may reduce NMB secretion, although TS% was within the normal range in individuals carrying the *NMBR* p.L390M in fasting conditions. Alternatively, NMB release may require intact NMBR and HFE dependent signaling. On the other hand, iron supplementation induced *NMBR* gene expression in HepG2 cells and in primary mouse hepatocytes *in vitro*. Consistently, chronic dietary iron overload resulted in upregulation of *Nmbr* in the liver, spleen and gut in mice.

Given the apparently discordant regulation of NMBR and NMB during chronic iron exposure, to better clarify whether the NMB-NMBR axis modulates hepcidin secretion and iron metabolism, we exposed primary murine hepatocytes to NMB with or without the NMBR antagonist PD168368, and evaluated the ability to modulate hepcidin induction by holo-transferrin. Indeed, NMBR can be modulated through the use of the antagonists, such as PD168368,[30] which have been tested in the field of oncology for their ability to block tumor growth and neo-vascularization.[49] Remarkably, NMB amplified hepcidin induction by holo-transferrin, and this amplification was completely abolished by PD168368, thereby suggesting that it is mediated by NMBR. Hepcidin induction was associated with upregulation of *Jak2* expression, which was completely abolished by PD168368. These data suggest that NMBR may be involved in mediating hepcidin release in hepatocytes by inducing JAK2, which can induce *HAMP* transcription by acting on STAT3 signaling.

Overall, consistently with the *in vivo* data during OITT, the results of this experiment suggest that the NMB-NMBR axis activation, likely by inducing JAK2, facilitates hepcidin release in response to the sudden rise in serum iron following intestinal absorption. Therefore, the association of *NMBR* mutations with iron overload might be mediated by a down-modulation of hepcidin release and JAK2 induction in response to iron. A hypothetical model of the role of the NMB-NMBR in the regulation of iron metabolism to be tested in future studies is shown in Figure 2. A down-modulation of NMB secretion induced by intestinal exposure to iron would permit its absorption by limiting hepcidin release (Figure 2, yellow panel). However, in the presence of excess of hepatic iron, this mechanism would be abolished due to increase of *NMBR* expression, which would increase iron induced hepcidin release, thereby limiting further absorption (Figure 2, green panel). Therefore, although the role of NMBR and JAK2 upregulation in limiting iron absorption in response to increased hepatic stores should be further confirmed in experimental models, *NMBR* and *JAK2* may represent potential targets for the treatment of iron state disorders.

Nevertheless, the present study suffers from some limitations. In particular, further experiments are needed to examine the impact of the p.L390M and other *NMBR* variants on protein expression, intracellular trafficking, and activity and on the regulation of intracellular signaling and iron metabolism. Furthermore, we could not evaluate whether *Nmbr* deletion modulates the susceptibility to iron overload in experimental models. Finally, the genetic association needs independent validation in larger cohort with individual patient data, to assess the impact on the diagnosis and risk stratification of primary iron overload disorders.

In conclusion, genetic and experimental data suggest that some *NMBR* mutations may predispose to iron accumulation by down-modulating hepcidin release in response to iron challenge in high risk individuals.

ACKNOWLEDGMENT

We thank all members of the Metabolic Liver Disease Center for helpful comments and discussion.

This study was supported by Fondazione Italiana per la Ricerca in Epatologia (FIRE) - ONLUS and Associazione Malattie Metaboliche del Fegato ONLUS (non-profit organizations for the study and care of metabolic liver diseases) and the Ricerca Corrente, Fondazione IRCCS Ca' Granda Milano (Institutional research funds, Public Research Institute). LV was supported by MyFirst Grant AIRC n.16888, Ricerca Finalizzata Ministero della Salute RF-2016-02364358, the European Union (EU) Programme Horizon 2020 (under grant agreement No. 777377) for the project LITMUS-"Liver Investigation: Testing Marker Utility in Steatohepatitis".

CONFLICT OF INTEREST

The authors declare no competing financial interests relevant to the present study.

ORCID

Raffaela Rametta https://orcid.org/0000-0003-0091-9394
Domenico Girelli https://orcid.org/0000-0001-9684-1899
Luca Valenti https://orcid.org/0000-0001-8909-0345

REFERENCES

1. Pietrangelo A. Genetics, genetic testing, and management of hemochromatosis: 15 years since hepcidin. *Gastroenterology*. 2015;149:1240-1251. e1244.
2. Pietrangelo A. Hereditary hemochromatosis: pathogenesis, diagnosis, and treatment. *Gastroenterology*. 2010;139:393-408.
3. Drakesmith H, Nemeth E, Ganz T. Ironing out ferroportin. *Cell Metab*. 2015;22:777-787.
4. Aschemeyer S, Qiao B, Stefanova D, et al. Structure-function analysis of ferroportin defines the binding site and an alternative mechanism of action of hepcidin. *Blood*. 2018;131:899-910.
5. Daher R, Kannengiesser C, Houamel D, et al. Heterozygous mutations in BMP6 Pro-peptide lead to inappropriate hepcidin synthesis and moderate iron overload in humans. *Gastroenterology*. 2016;150:672-683.e4.

6. Piubelli C, Castagna A, Marchi G, et al. Identification of new BMP6 pro-peptide mutations in patients with iron overload. *American Journal of Hematology*. 2017;92:562-568.
7. Carella M, D'Ambrosio L, Totaro A, et al. Mutation analysis of the HLA-H gene in Italian hemochromatosis patients. *Am J Med Genet*. 1997;60:828-832.
8. Fracanzani AL, Piperno A, Valenti L, et al. Hemochromatosis in Italy in the last 30 years: role of genetic and acquired factors. *Hepatology*. 2010;51:501-510.
9. Pietrangelo A. Pathogens, metabolic adaptation, and human diseases–an iron-thrifty genetic model. *Gastroenterology*. 2015;149:834-838.
10. Benyamin B, Ferreira MA, Willemsen G, et al. Common variants in TMPRSS6 are associated with iron status and erythrocyte volume. *Nat Genet*. 2009;41:1173-1175.
11. Nai A, Pagani A, Silvestri L, et al. TMPRSS6 rs855791 modulates hepcidin transcription in vitro and serum hepcidin levels in normal individuals. *Blood*. 2011;118:4459-4462.
12. Valenti L, Fracanzani AL, Rametta R, et al. Effect of the A736V TMPRSS6 polymorphism on the penetrance and clinical expression of hereditary hemochromatosis. *J Hepatol*. 2012;57:1319-1325.
13. McLaren CE, Emond MJ, Subramaniam VN, et al. Exome sequencing in HFE C282Y homozygous men with extreme phenotypes identifies a GNPAT variant associated with severe iron overload. *Hepatology*. 2015;62:429-439.
14. Greni F, Valenti L, Mariani R, et al. GNPAT rs11558492 is not a major modifier of iron status: study of italian hemochromatosis patients and blood donors. *Annals of Hepatology*. 2017;16:451-456.
15. Ryan E, Russell J, Ryan JD, Crowe J, Stewart S. GNPAT variant is not associated with severe iron overload in Irish C282Y homozygotes. *Hepatology*. 2016;63:2055-2056.
16. Badar S, Busti F, Ferrarini A, et al. Identification of novel mutations in hemochromatosis genes by targeted next generation sequencing in Italian patients with unexplained iron overload. *Am J Hematol*. 2016;91:420-425.
17. Valenti L, Rametta R, Dongiovanni P, et al. The A736V TMPRSS6 polymorphism influences hepatic iron overload in nonalcoholic fatty liver disease. *PLoS One*. 2012;7:e48804.
18. Ryan JD, Armitage AE, Cobbold JF, et al. Hepatic iron is the major determinant of serum ferritin in NAFLD patients. *Liver Int*. 2018; 38:164-173.
19. Rametta R, Dongiovanni P, Pelusi S, et al. Hepcidin resistance in dysmetabolic iron overload. *Liver Int*. 2016;36:1540-1548.
20. Li H, Deng H. Systems genetics, bioinformatics and eQTL mapping. *Genetica*. 2010;138:915-924.
21. McKenna A, Hanna M, Banks E, et al. The genome analysis toolkit: a MapReduce framework for analyzing next-generation DNA sequencing data. *Genome Res*. 2010;20:1297-1303.
22. DePristo MA, Banks E, Poplin R, et al. A framework for variation discovery and genotyping using next-generation DNA sequencing data. *Nat Genet*. 2011;43:491-498.
23. Van der Auwera GA, Carneiro MO, Hartl C, et al. From FastQ data to high confidence variant calls: the genome analysis toolkit best practices pipeline. *Curr Protoc Bioinformatics*. 2013;43:11.10.1-11.10.33.
24. McLaren W, Gil L, Hunt SE, et al. The ensembl variant effect predictor. *Genome Biol*. 2016;17:122.
25. Genomes Project C, Auton A, Brooks LD, et al. A global reference for human genetic variation. *Nature*. 2015;526:68-74.
26. Lek M, Karczewski KJ, Minikel EV, et al. Analysis of protein-coding genetic variation in 60,706 humans. *Nature*. 2016;536:285-291.
27. Kircher M, Witten DM, Jain P, O'Roak BJ, Cooper GM, Shendure J. A general framework for estimating the relative pathogenicity of human genetic variants. *Nat Genet*. 2014;46:310-315.
28. Quang D, Chen Y, Xie X. DANN: a deep learning approach for annotating the pathogenicity of genetic variants. *Bioinformatics*. 2015;31:761-763.
29. Mederacke I, Dapito DH, Affo S, et al. High-yield and high-purity isolation of hepatic stellate cells from normal and fibrotic mouse livers. *Nature Protocols*. 2015;10:305-315.
30. Ryan RR, Katsuno T, Mantey SA, et al. Comparative pharmacology of the nonpeptide neuromedin B receptor antagonist PD 168368. *J Pharmacol Exp Ther*. 1999;290:1202-1211.
31. Dongiovanni P, Ruscica M, Rametta R, et al. Dietary iron overload induces visceral adipose tissue insulin resistance. *Am J Pathol*. 2013;182:2254-2263.
32. Corjay MH, Dobrzanski DJ, Way JM, et al. Two distinct bombesin receptor subtypes are expressed and functional in human lung carcinoma cells. *J Biol Chem*. 1991;266:18771-18779.
33. Moody TW, Fagarasan M, Zia F. Neuromedin B stimulates arachidonic acid release, c-fos gene expression, and the growth of C6 glioma cells. *Peptides*. 1995;16:1133-1140.
34. Dobrzanski D, Sharoni Y, Wada E, Battey J, Sausville E. Neuromedin-B receptor transfected BALB/3 T3 cells: signal transduction and effects of ectopic receptor expression on cell growth. *Regul Pept*. 1993;45:341-352.
35. Benya RV, Kusui T, Pradhan TK, Battey JF, Jensen RT. Expression and characterization of cloned human bombesin receptors. *Mol Pharmacol*. 1995;47:10-20.
36. Hou W, Tsuda T, Jensen RT. Neuromedin B activates phospholipase D through both PKC-dependent and PKC-independent mechanisms. *Biochim Biophys Acta*. 1998;1391:337-350.
37. Severi C, Jensen RT, Erspamer V, et al. Different receptors mediate the action of bombesin-related peptides on gastric smooth muscle cells. *Am J Physiol*. 1991;260:G683-G690.
38. Pazos-Moura CC, Moura EG, Rettori V, Polak J, McCann SM. Role of neuromedin B in the in vitro thyrotropin release in response to thyrotropin-releasing hormone from anterior pituitaries of eu-, hypo-, and hyperthyroid rats. Proceedings of the Society for Experimental Biology and Medicine Society for. *Exp Biol Med*. 1996;211:353-358.
39. Ortiga-Carvalho TM, Oliveira Kde J, Morales MM, Martins VP, Pazos-Moura CC. Thyrotropin secretagogues reduce rat pituitary neuromedin B, a local thyrotropin release inhibitor. *Exp Biol Med*. 2003;228:1083-1088.
40. Ladenheim EE, Taylor JE, Coy DH, Moran TH. Blockade of feeding inhibition by neuromedin B using a selective receptor antagonist. *Eur J Pharmacol*. 1994;271:R7-R9.
41. Merali Z, McIntosh J, Anisman H. Role of bombesin-related peptides in the control of food intake. *Neuropeptides*. 1999;33:376-386.
42. Ohki-Hamazaki H, Sakai Y, Kamata K, et al. Functional properties of two bombesin-like peptide receptors revealed by the analysis of mice lacking neuromedin B receptor. *J Neurosci*. 1999;19:948-954.
43. Merali Z, Kent P, Anisman H. Role of bombesin-related peptides in the mediation or integration of the stress response. *Cell Mol Life Sci*. 2002;59:272-287.
44. Merali Z, Bedard T, Andrews N, et al. Bombesin receptors as a novel anti-anxiety therapeutic target: BB1 receptor actions on anxiety through alterations of serotonin activity. *J Neurosci*. 2006;26:10387-10396.
45. Moody TW, Staley J, Zia F, Coy DH, Jensen RT. Neuromedin B binds with high affinity, elevates cytosolic calcium and stimulates the growth of small-cell lung cancer cell lines. *J Pharmacol Exp Ther*. 1992;263:311-317.
46. Siegfried JM, Krishnamachary N, Gaither Davis A, Gubish C, Hunt JD, Shriver SP. Evidence for autocrine actions of neuromedin B and

gastrin-releasing peptide in non-small cell lung cancer. *Pulm Pharmacol Ther*. 1999;12:291-302.
47. Matusiak D, Glover S, Nathaniel R, Matkowskyj K, Yang J, Benya RV. Neuromedin B and its receptor are mitogens in both normal and malignant epithelial cells lining the colon. *Am J Physiol Gastrointest Liver Physiol*. 2005;288:G718-G728.
48. Bouchard L, Drapeau V, Provencher V, et al. Neuromedin beta: a strong candidate gene linking eating behaviors and susceptibility to obesity. *Am J Clin Nutr*. 2004;80:1478-1486.
49. Park HJ, Kim SR, Kim MK, et al. Neuromedin B receptor antagonist suppresses tumor angiogenesis and tumor growth in vitro and in vivo. *Cancer Lett*. 2011;312:117-127.

SUPPORTING INFORMATION

Additional supporting information may be found online in the Supporting Information section at the end of this article.

How to cite this article: Rametta R, Dongiovanni P, Baselli GA, et al. Impact of natural neuromedin-B receptor variants on iron metabolism. *Am J Hematol*. 2020;95:167–177. https://doi.org/10.1002/ajh.25679